Iranian Journal of Chemical Engineering

Journal Homepage: www.ijche.com

pISSN: 1735-5397
eISSN: 2008-2355

Experimental Measurement and Thermodynamic Modeling of CO_2 Absorption in a Wide Range of Aqueous MDEA Solutions (10-98 wt%)

Mohammad Saleh Sedighi[1], Hassan Pahlavanzadeh[2,*], Mehdi Ardjmand[1], Mahdi Goharrokhi[1]

[1]*Department of Chemical Engineering, South Tehran Branch, Islamic Azad University, Tehran, Iran*
[2]*Faculty of Chemical Engineering, Tarbiat Modares University, Tehran, Iran*

ARTICLE INFO

Article type:
Research article

Article history:
Received: 2024-03-29
Revised: 2024-07-27
Accepted: 2024-08-24
Available online: 2024-09-24

Keywords:
Vapor-liquid equilibria,
CO_2 absorption,
MDEA,
Experimental measurement,
Thermodynamic modeling

ABSTRACT

In this study, the process of capturing CO_2 by using an aqueous MDEA solution under the operating conditions of the concentration range of 10-98 wt% of MDEA, temperature range of 303-323K and atmospheric pressure is investigated. Most researchers have measured the effect of pressure changes on the loading, but in this work, we have investigated the effect of changing the concentration of amine on the loading. We employed the apparatus introduced by Pahlavanzadeh et al. to evaluate the solubility of carbon dioxide in the aqueous solutions of N-methyldiethanolamine (MDEA). The results indicate that the maximum absorption of CO_2 takes place in concentration of between 40-50 wt% of MDEA. Subsequently, the Cubic-Two-State Equation of State (CTS EoS) was improved and used to describe the solubility of CO_2 in aqueous MDEA solutions in a wide range of concentrations and temperatures. This equation, referred to as CTS^{DH}, includes three terms relating to the different intermolecular interactions happening in electrolyte solutions. The same EoS was used for vapor and liquid phases. Model parameters were adjusted according to the experimental results of this work and other researches. Using the adjustable parameters from this work, the model successfully approximated CO_2 loading under a wide range of functional conditions. The evaluation of model results with experimental data showed the average absolute percent deviation (AAD%) to be 7.05%, indicating a satisfactory alignment between model predictions and Measured results.

DOI: 10.22034/ijche.2024.450400.1526 URL: https://www.ijche.com/article_206316.html

*Corresponding author: pahlavzh@modares.ac.ir

1. Introduction

Global warming is one of the consequences of greenhouse gas (GHG) emissions. Therefore, reducing the production and controlling the emission of these gases is considered an international and environmental approach. The process of removing acid gases (CO_2, H_2S) from industrial gases and natural gas, which is called sweetening, is often done by amine solvents. In this process, acid gases are converted into ionic species during a series of equilibrium chemical reactions that take place in the presence of amine solvents in the liquid phase. Due to its lower thermal decomposition, vapor pressure, and corrosion, N-methyl diethanolamine (MDEA) is better and more effective than other amine solvents. The equilibrium calculations of such systems are complicated due to the production of numerous ionic species and must be performed by thermodynamic models. In general, the models, which are used, can be divided into three categories:

i. Semi-empirical models: In these models, ideal gas and liquid phases are considered. The equilibrium coefficients of chemical reactions and Henry's law coefficients are adjustable parameters. The Kent-Eisenberg[1] model is one of the most famous semi-empirical ones.

ii. (γ – φ) approach models: In these models, the non-ideality of gas and liquid phases is described by an equation of state and activity coefficient model. The most important problem of these models is the lack of the influence of pressure on activity coefficients and the density calculation. Posey and Rochelle[2] described the thermodynamic behavior of the system (H_2O-MDEA-CO_2) using the NRTL model. To model the vapor-liquid equilibrium (VLE), they used thermodynamic and equilibrium data simultaneously and introduced a new function. Deshmukh and Mather[3] also obtained a model to describe the solubility of acid gases in the MEA aqueous solution by integrating Pitzer and Debye-Hückel models.

iii. (φ – φ) approach models: In these models, the non-ideal behavior of gas and liquid phases is described by an equation of state. Since the parameters used to fit the model with the experimental data are numerous, the models with the (φ – φ) approach are more attractive than others. Fürst and Renon[4] expanded the Helmholtz free energy expression to describe the behavior of electrolyte solutions, and obtained a new equation of state that included a non-electrolyte part and an ionic part. By adding a born term to Fürst and Renon's equation, Huttenhuis et al.[5,6] attained at a new equation for the vapor-liquid equilibrium calculations of the system (H_2O-MDEA-CH_4-CO_2). Also, Myers et al.[7] obtained an equation based on Helmholtz free energy, which included three sections Peng-Robinson, born, and mean spherical approximation. In other studies, Sadowski et al.[8-12] developed the PC-SAFT equation of state and were able to model the phase equilibrium (VLE-LLE-SLE) of three-component electrolyte solutions with a high approximation. Medeiros and Téllez[13] presented the Cubic-Two-State (CTS) Equation of State for Associating Fluids. They also made excellent predictions of multicomponent systems, by combining CTS EoS with an electrolyte model[14]. All these models have a common feature: the pair of an electrolytic term with a non-electrolyte EoS.

In this work, a combination of the Cubic-Two-State (CTS) EoS and the Debye-Hückel[15-18] model is used to predict the thermodynamic behavior of the system (H_2O-MDEA-CO_2).

2. Experimental section

2.1. Materials

MDEA was purchased from Merck with the purity of 98% and CO_2 from Sohail Gas Industrial Group. The characteristics of the

materials used in this research are presented in Table (1). To prepare the solvents in the desired concentrations, we used a digital balance (AND, HR-250A) with an accuracy of ± 0.1 milligrams for the measurement of the weight of MDEA and H_2O.

Table 1.
Specifications, sources and purity of materials used in this work.

Chemical Name	Formula	Abbreviation	Supplier	Purity
N-Methyldiethanolamine	$C_5H_{13}NO_2$	MDEA	Merck	98%
Carbon Dioxide	CO_2	CO_2	Soheil Gas Industrial Group	99.995%

2.2. Apparatus

The first step in determining the solubility of gases in liquids is the contact of the solvent and the solute with each other until the saturation state is reached. Therefore, under the test conditions (known temperature and pressure), it is possible to calculate the molar volume and moles of the gas dissolved in the solvent by a simple equation of state. Since the mole of solvent is already known to us, it is easy to calculate the amount of solubility. Pahlavanzadeh et al.[19,20] designed and used an apparatus to determine the solubility of gases in liquids and a similar apparatus was used in this work. This apparatus is shown in Fig. (1) and includes the following parts:

i. Spiral tube: This section consists of a spiral tube with a certain number of screws. The liquid phase is saturated with gas through this passage. By changing the type of solvent and solute, the diameter, slope, and number of screws change. If the solubility of the gas is high, designing more screws and reducing the slope help us to reach the equilibrium of solvent and solute at the end of the spiral tube.

ii. Scaling burette: The Scaling burette is used to store the gas inside the device and also to estimate the volume of the gas dissolved in the solvent. The top of the burette is connected to the spiral tube and the bottom to a valve. This valve is connected on one side to the CO_2 cylinder and on the other side to a mercury vessel. The mercury container is placed on a movable jack so that the height of the solution inside the manometer can be adjusted.

iii. Manometer: A manometer is placed at the end of the spiral tube to show pressure changes. The other end of this manometer is open to the atmosphere.

iv. Syringe pump: The injection of the solvent inside the spiral tube at a constant speed is done by a syringe pump. The syringe pump consists of a mini-computer, to control the injection speed, and a mechanical part.

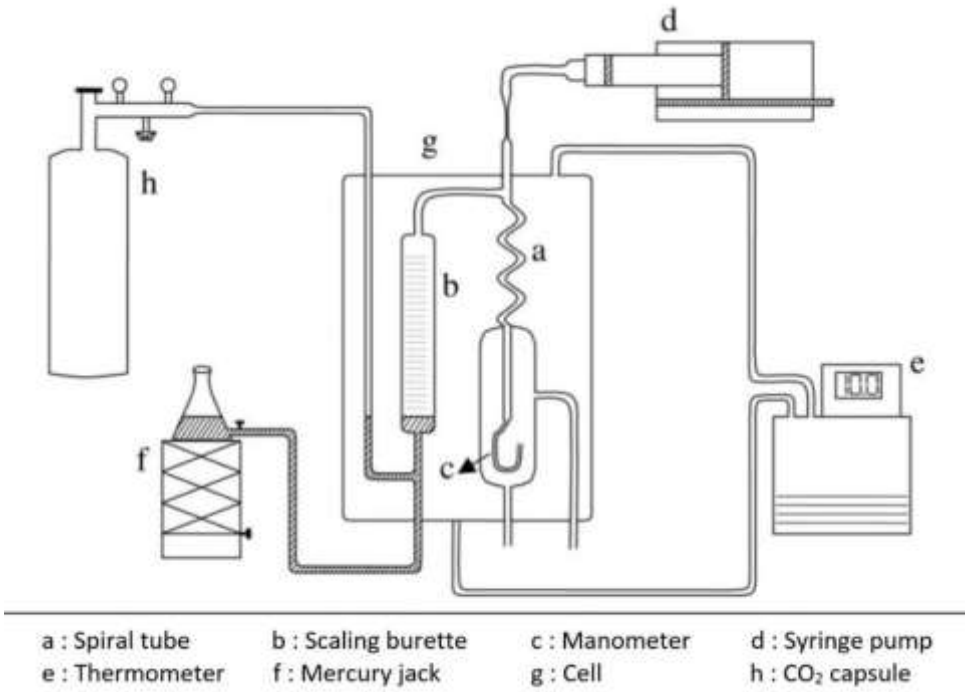

Figure 1. Apparatus for measuring the solubility of the gas in the liquid.

3. Thermodynamic modeling section

The aim of this work is to investigate the amount of the absorption of carbon dioxide in an aqueous MDEA solution and to model the behavior of this system. To determine the concentration of each component in this system, it is necessary to simultaneously solve the chemical and phase equilibrium equations.

3.1 Chemical equilibrium

The following reactions handled the chemical equilibrium of CO_2 in aqueous MDEA solutions:

$$H_2O \xleftrightarrow{K1} H^+ + OH^- \qquad K_1 = \frac{[H^+]\,[OH^-]}{[H_2O]}\,\frac{\gamma_{H^+}\ \gamma_{OH^-}}{\gamma_{H_2O}} \qquad R_1$$

$$H_2O + CO_2 + \xleftrightarrow{K2} H^+ + HCO_3{}^- \qquad K_2 = \frac{[H^+]\,[HCO_3^-]}{[H2O]\,[CO_2]}\,\frac{\gamma_{H^+}\ \gamma_{HCO_3^-}}{\gamma_{H_2O}\ \gamma_{CO_2}} \qquad R_2$$

$$HCO_3{}^- \xleftrightarrow{K3} H^+ + CO_3{}^{-2} \qquad K_3 = \frac{[H^+]\,[CO_3^{2-}]}{[HCO_3^-]}\,\frac{\gamma_{H^+}\ \gamma_{CO_3^{2-}}}{\gamma_{HCO_3^-}} \qquad R_3$$

$$MDEAH^+ \xleftrightarrow{K4} MDEA + H^+ \qquad K_4 = \frac{[M]\,[H^+]}{[M^+]}\,\frac{\gamma_M\ \ \gamma_{H^+}}{\gamma_{M^+}} \qquad R_4$$

The chemical equilibrium constants of reactions R_1-R_4 are defined by Eq. (1).

$$K_j(T) = \prod_i (x_i\gamma_i)^{v_{ij}} = \mathrm{Exp}\left(C_1 + \frac{C_2}{T} + C_3 LnT\right) \qquad (1)$$

In Eq. (1), K_j is the equilibrium constant of reaction R_j, γ_i the activity coefficient of species i, and v_{ij} is the stoichiometric coefficient of substance i in reaction R_j. The numerical values of coefficients C_1-C_3 in Eq. (1) for all reactions are given in Table (2).

Table 2.
Coefficients for calculating chemical Equilibrium Constants, Eq. (1).

Reaction	C_1	C_2	C_3	T(K)	Reference
R.1	132.899	-13445.9	-22.4773	273–498	[5,6]
R.2	231.465	-12092.1	-36.7816	273–498	[5,6]
R.3	216.049	-12431.7	-35.4819	273–498	[5,6]
R.4	-77.262	-1116.5	10.06	278–423	[5,6]
Henry's law	$H_{CO2} = Exp\left(\frac{-6789\square04}{T} - 11\square4519 * lnT - 0\square010454T + 94\square4914\right)$				[34]

3.2 Phase equilibrium

One of the most important quantities that must be calculated in phase equilibrium calculations is the fugacity coefficient. Activity coefficients are usually needed to do phase equilibrium calculations in electrolyte systems. The activity coefficients are derived from fugacity coefficients. The mole fraction-based activity coefficient of solvents (H_2O and MDEA) in an electrolyte solution is defined as the ratio of the fugacity coefficient of component i in the solution to the fugacity coefficient of pure component i. The activity coefficient for the solvent is defined by Eq. (2):

$$\gamma_i = \frac{\varphi_i(T.P.x_i)}{\varphi_i^{Pure}(T.P.x_i \to 1)}. \qquad i = water\ .\ MDEA \quad (2)$$

For solutes (acid gases and ionic species), activity coefficients are determined by Eq. (3):

$$\gamma_i = \frac{\varphi_i(T.P.x_i)}{\varphi_i^{\infty}(T.P.x_i \to 0.x_{solvent} \to 1)}\ . \qquad i = CO_2\ .\ ions \quad (3)$$

Where φ_i is the fugacity coefficients of component i under system conditions, φ_i^{Pure} is the fugacity coefficient of water and MDEA under Pure conditions and φ_i^{∞} is the fugacity coefficient of CO_2 and ions under infinitely dilute conditions. Fugacity coefficients of ionic and molecular species in all conditions are calculated by CTS^{DH} EoS. Also, it is assumed that ionic species are only present in the liquid phase. The activity coefficients of the H_3O^+ and OH^- ions are set at unity because they have very low concentrations ($\gamma_{H_3O^+} = 1\ .\ \gamma_{OH^-} = 1$). At a temperature range of 298 to 413 K, the vapor pressure of MDEA is very low, so it is assumed that this substance does not exist in the vapor phase, and the vapor phase includes only CO_2 and H_2O. In addition to chemical and phase equilibrium equations, mass balance and charge balance equations are needed to determine the controlling system of equations. These relationships are presented in Eqs. (4-8).

Charge Balance :

$$[H^+] + [M^+] = [OH^-] + [HCO_3^-] + 2[CO_3^=] \quad (2)$$

Total CO_2 Balance :

$$[CO_2]_t = [CO_2] + [HCO_3^-] + [CO_3^=] \quad (3)$$

Total MDEA Balance :

$$[m]_t = [MDEA] + [MDEAH^+] \quad (4)$$

Henry's law :

$$P_{CO_2} = H_{CO_2}[CO_2]\,\gamma_{CO_2} \quad (5)$$

CO_2 Loading :

$$\alpha = \frac{[CO_2]_t}{[m]_t} \to [m]_t\ \alpha = [CO_2] + [HCO_3^-] + [CO_3^=] \quad (6)$$

3.3. CTS^{DH} EoS

The values of the fugacity coefficients of the components in the gas and liquid phases are determined by the EoS. In this work, the equation of state presented by Medeiros et al., of which the electrolytic part has been improved, is used. This equation is composed of a non-associative part (described by SRK EoS[21]), an associative part (described by TSAM[22]), and an electrolytic part (described by Debye-Hückel[18]), in order to predict the behavior of such systems. As mentioned, CTS

EoS is improved in the electrolytic part and CTS^{DH} EoS is obtained as per Eq. (9):

$$P^{CTS^{DH}}(x.v.T) = \frac{RT}{v-b(x)} - \frac{a(x.T)}{v[v+b(x)]} - RT\sum_i^{n_c} x_i \frac{\sum_j^{n_c} x_j v_{ij} f_{ij}(T)}{v[v+\sum_j^{n_c} x_j v_{ij} f_{ij}(T)]} - \frac{\kappa F^2}{24 N_A \pi \varepsilon}\sum_i^{n_c} x_i\, \sigma_i \hat{z}_i^2 \quad (6)$$

Where, x_i and x_j are the molar fractions of species i and j respectively, n_c is the number of components in the mixture, f_{ij} is the Mayer function defined in Eq. (10), Ƙ is the inverse Debye screening length defined in Eq. (11), F is the Faraday constant, N_A is the Avogadro's constant, ε is the Dielectric constant of the system, σ_i is the ion diameter and $\hat{z}_i$ is the charge number of ion i.

$$f_{ij} = \exp -\left(E_{ij} \,/\, RT\right) - 1 \quad (7)$$

$$\kappa^2 = \frac{\rho_N e^2}{K_B T \varepsilon}\sum_i x_i \hat{z}_i^2 \quad (8)$$

In equation (10), E_{ij} and V_{ij} are the energy and the characteristic volume of association for each type of association that could occur respectively. In equation (11), ρ_N is the number of density, e is the elementary charge and K_B is the Boltzmann constant. Therefore, the fugacity coefficient of each component in the system is obtained by the Eq. (12).

$$\begin{aligned} ln\varphi_i = {} & \frac{B_i'}{B}(Z-1) - \ln(Z-B) + \frac{A}{B}\left(\frac{A_i'}{A} - \frac{B_i'}{B}\right) ln\left(\frac{Z}{Z+B}\right) && \text{(SRK Term)} \\ & + ln\left(\frac{Z}{Z+\sum_{j=1}^{n_c} x_j\, C_{ij}}\right) - \sum_{k=1}^{n_c}\left(\frac{x_k C_{ki}}{Z+\sum_{j=1}^{n_c} x_j C_{kj}}\right) && \text{(Association Term)} \\ & - \frac{\kappa F^2 \hat{z}_i^2}{24 N_A \pi \varepsilon RT}\left(\frac{\sum_j x_j \sigma_j\, \hat{z}_j^2}{\sum_j x_j \hat{z}_j^2} + 2\mathbb{X}_i\right) - \ln(Z) && \text{(Debye} - \text{Hückel Term)} \\ f_i = {} & \varphi_i\, P_t \end{aligned} \quad (9)$$

Where φ_i and f_i are the fugacity coefficient and fugacity of component i respectively. The relationships related to SRK and Association terms presented by Medeiros et al. have been used exactly in this work. The relationships related to the Debye-Hückel term are also presented below:

In the Debye-Hückel Term of Eq. (12), x_i is the mole fraction of ion i, and quantity $\mathbb{X}_i$ is defined as Eq. (13):

$$\mathbb{X}_i = \frac{3}{(\kappa\sigma_i)^3}\left[\frac{3}{2} + \ln(1+\kappa\sigma_i) - 2(1+\kappa\sigma_i) + \frac{1}{2}(1+\kappa\sigma_i)^2\right] \quad (10)$$

The dispersion energy function for ionic species is defined by Eq. (14):

$$a_{ii}(T) = (d_1 - d_2 T^{0.5})^2 \quad (11)$$

Where d_1 and d_2 are adjustable parameters. Through six pure component parameters (b, d_1, d_2, V_{ii}, E_{ii}) and (σ_{ij}) which are respectively related to CTS and the long-range ion-ion contribution, CTS^{DH} EoS will be able to describe systems in which there are associational and electrolyte interactions.

4. Results and discussion

4.1. Experimental results

The solubility of CO_2 in 10-98 wt% of MDEA solutions was measured at the temperatures of 303-323K and atmospheric pressure. To measure the solubility of the gas, first, the solvent with the desired concentration was prepared. Then the device was filled with gas and ready to inject the solvent. The injection of the mixed solvent into the spiral tube was done slowly and with a constant flow rate of 2.511 ml/hr. This flow rate was chosen after preliminary tests and ensuring that the solvent was saturated by the gas. As soon as the first droplet of the solution reached the u-shaped manometer, the solute gas flow was blocked by increasing the height of the mercury vessel. As the gas dissolved in the solvent, the pressure inside the devicedecreased. The pressure drop was controlled by increasing the height of the mercury vessel so that the pressure of the device would remain constant during the test. In the end, the amount of the gas dissolved in the solvent was obtained from the volume of mercury displaced. In each test, the solubility of the gas was determined by recording the volume of mercury displaced and the elapsed time. Using Eq. (15), the number of the moles of CO_2 dissolved in the MDEA solution can be calculated:

$$n_{CO_2} = \frac{V_{CO_2}}{\mathrm{U}_{m.CO_2}} \tag{12}$$

Where V_{CO2} is the displaced volume of mercury in the burette during the test and $\mathrm{U}_{m,CO2}$ is the molar volume of CO_2 under test conditions, which is calculated by the simple equation of state. Also, the total moles of the solution (H_2O+MDEA) is obtained fromEq. (16):

$$n_t = \frac{Q\ t\ \rho_{mix}}{M_{w.mix}} \quad . \quad n_{MDEA} = n_t \frac{\%Wt_{MDEA}}{100} \tag{13}$$

Where Q is the Volumetric flow rate of the injectable solvent, t is the solubility time, and ρ_{mix} and $M_{w,mix}$ are the density and molecular weight of the aqueous MDEA solution respectively. Finally, the Experimental loading (α_{exp}) is obtained from Eq. (17):

$$\alpha_{exp} = \frac{n_{CO_2}}{n_{MDEA}} \tag{14}$$

To ensure the correctness of the results and increase their accuracy, each test was performed three times and their average was considered as the final result. The results of the dissolved gas volume at the specific concentrations of solvent at different temperatures are presented in Table (3). In this table, V_{CO2} is the volume of CO_2 dissolved in the solvent during the test and n_{MDEA} is the number of the moles of MDEA injected into the system. Also, the volumetric flow rate is constant for all tests, but the mass flow rate is different for each experiment due to changes in density and concentration.

Table 3.
Solubility of Carbon Dioxide in the Aqueous Solutions of MDEA. (Measured in this work).

T (K)	Wt% MDEA	V_{CO2} (cm^3)	n CO2	n MDEA	α
303.15	10	19	0.000764	0.000702	1.088
	20	35	0.001407	0.001409	0.999
	30	47	0.001889	0.002121	0.891
	40	54	0.002171	0.002838	0.765
	50	51	0.002050	0.003560	0.576
	60	40.5	0.001628	0.004288	0.380
	80	24.5	0.000985	0.005758	0.171
	98	19	0.000764	0.007099	0.108
313.15	10	18	0.000700	0.000699	1.002
	20	31	0.001206	0.001403	0.860
	30	40.5	0.001576	0.002111	0.746
	40	46	0.001790	0.002824	0.634
	50	43	0.001673	0.003542	0.472
	60	35	0.001362	0.004264	0.319
	80	22	0.000856	0.005722	0.150
	98	15	0.000584	0.007049	0.083
323.15	10	16.5	0.000622	0.000696	0.894
	20	27	0.001018	0.001396	0.739
	30	35	0.001320	0.002101	0.628
	40	38	0.001433	0.002809	0.510
	50	36.5	0.001376	0.003522	0.391
	60	30	0.001131	0.004238	0.267
	80	19	0.000717	0.005684	0.126
	98	10	0.000377	0.006999	0.054

The volumetric flow rate of injectable solvent : Q°= 0.04185 Cm^3/min

Duration of all Experimental tests : time = 20 min

Total Pressure : P_t = 101.325 Kpa

The experimental loadings of CO_2 in MDEA solutions at various temperatures are presented in Fig. (2). This figure shows that, as expected, the loading decreased by increasing temperature, which can be a confirmation of the correct procedure of conducting experimental studies in this work.

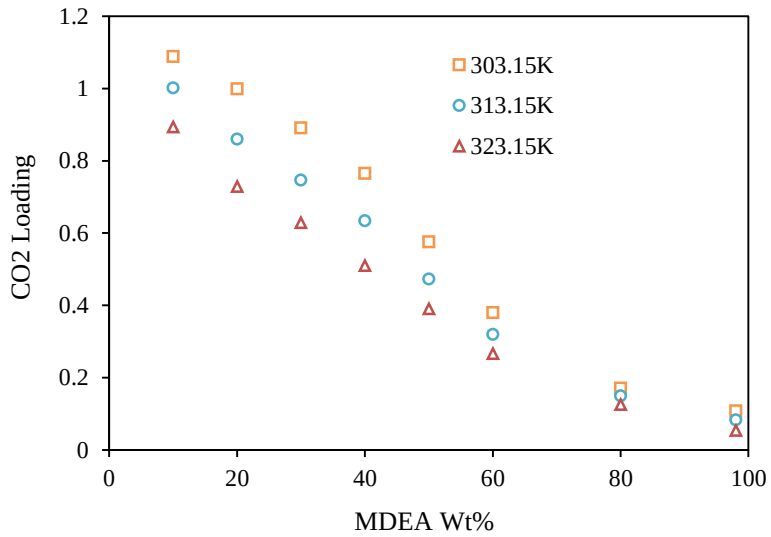

Figure 2. Experimental CO_2 loading in the aqueous solutions of MDEA. (Measured in this work)

As shown in Fig. (3), the maximum moles of CO_2 were absorbed in MDEA with the concentration of 40-50 wt%, which increased from about 40% to about 50% as the temperature increased from 303K to 323K. Therefore, it can be said that the optimal concentration of MDEA increases slowly by increasing temperature. At high concentrations of MDEA, the pH of the solution is very high. Therefore, free MDEA molecules act as the base that accepts protons from HCO_3^- and forms $CO_3^=$, leading to an increase in the concentration of $CO_3^=$. At low concentrations of MDEA, the PH decreases, which causes $CO_3^=$ to accept protons to form HCO_3^-, causing to decrease the concentration of $CO_3^=$. MDEA as a tertiary amine does not produce carbamate. By the formation of HCO_3^- and $MDEAH^+$, CO_2 is absorbed by MDEA.

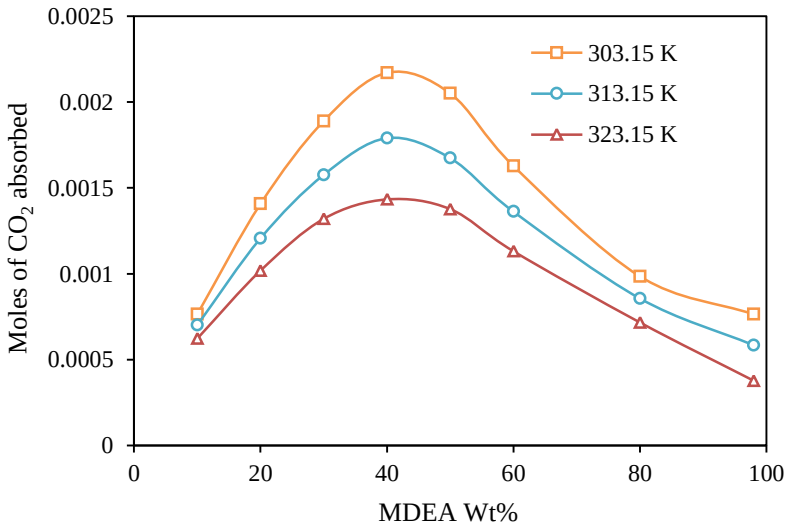

Figure 3. Number of the moles of CO_2 absorbed in the MDEA solution with different concentrations (Measured in this work).

4.2. Modeling results

In the first step of modeling, vapor pressure, and saturated liquid density data are included in the regression. in this way adjusting the associating pure component parameters is done. In the second step, the vapor-liquid equilibrium calculations were done to adjust the molecular binary interaction parameters. Finally, the solubility of the gas in the liquid was determined by adjusting molecular and ionic binary interaction parameters and simultaneously solving chemical and phase equilibrium equations. The results show that the model was able to provide a relatively good CO_2 loading under a wide range of operating conditions. The comparison of the experimental loading and the calculated loading obtained in this work, as well as the average absolute percent deviation (AAD%) between them, is shown in Table (4).

Table 4.
Comparison of experimental (measured in this work) and model (calculated by CTS^{DH}) CO_2 loadings in the H_2O-MDEA-CO_2 system at various temperatures and MDEA concentrations.

T (K)	Wt% $_{MDEA}$	α Exp	α Cal	Error %
303.15	10	1.088	1.053	3.3
	20	0.999	1.002	0.3
	30	0.891	0.881	1.1
	40	0.765	0.697	8.9
	50	0.576	0.516	10.4
	60	0.380	0.347	8.6
	80	0.171	0.192	12.2
	98	0.108	0.089	17.3
313.15	10	1.002	1.020	1.8
	20	0.860	0.947	10.1
	30	0.746	0.820	9.8
	40	0.634	0.636	0.3
	50	0.472	0.432	8.6
	60	0.319	0.293	8.3
	80	0.150	0.147	1.8
	98	0.083	0.076	8.2
323.15	10	0.894	0.939	5.1
	20	0.739	0.810	9.6
	30	0.628	0.679	8.1
	40	0.510	0.537	5.3
	50	0.391	0.384	1.8
	60	0.267	0.273	2.3
	80	0.126	0.140	11.1
	98	0.054	0.062	15.1
AAD %				**7.05**

α Exp: Measured in this work
α Cal: Calculated by CTS^{DH} EoS

4.2.1. Pure component parameters

A_{0i}, b_i, c_i, V_{ii}, and E_{ii} are adjustable parameters for pure associating components, and b_i, V_{ii}, E_{ii}, d_1, d_2, and σ_i are adjustable parameters for ionic species. These parameters are determined by fitting the model with experimental data from other papers. The values of the adjusted parameters for the pure components and the average absolute deviation of the vapor pressure and saturated liquid density from the experimental data are presented in Table (5). In this work, the method of which the algorithm is explained in Fig. (4) is used to minimize the objective function presented in Eqs. (18, 19). The % AAD of the model compared to the experimental data for H_2O, MDEA and CO_2 is 0.7, 0.76 and 0.78 respectively. The experimental data for Pure H_2O and CO_2 were taken from the Design Institute of Physical Properties DIPPR database[23] and Experimental data for MDEA were calculated using the correlation presented by Kontogeorgis et al.[24]. The diameter of ionic species ($MDEAH^+$, HCO_3^-, and $CO_3^=$) proposed by Huttenhuis et al. (2008) was used in this work. Table (5) shows these correspondences.

$$OF_{Pure}(a_{0i}.b_i.c_{1i}.v_{ii}.E_{ii}) = \sum\left(\frac{P_s^{calc}-P_s^{exp}}{P_s^{exp}}\right)^2 + \sum\left(\frac{\rho_s^{calc}-\rho_s^{exp}}{\rho_s^{exp}}\right)^2 = Minimize \quad (15)$$

Table 5.
Pure component parameters of the CTS^{DH}.

	H_2O	MDEA	CO_2	$MDEAH^+$	HCO_3^-	$CO_3^=$
M_w [kg/kmol]	18.02	119.16	44.01	120.16	61.00	59.98
Tc [K]	647.3 [a]	677.0 [a]	304.2 [a]	-	-	-
Pc [Mpa]	22.09 [a]	3.88 [a]	7.4 [a]	-	-	-
ω	0.344 [a]	1.242 [a]	0.224 [a]	-	-	-
a_0 [Pa.m^6/mol^2]	0.387 [b]	3.411 [b]	0.332 [b]	-	-	-
b × 10^6 [m^3/mol]	14.78 [b]	104.81 [b]	27.91 [b]	114.31 [b]	26.17 [b]	21.13 [c]
c_1	0.576 [b]	0.802 [b]	0.718 [b]	-	-	-
V_{ii} × 10^6 [m^3/mol]	1.12 [b]	0.981 [b]	0.819 [b]	0.389 [b]	0.318 [b]	0.827 [c]
$-E_{ii}$ / R [K]	1283.52 [b]	2449.74 [b]	394.03 [b]	3782.39 [b]	910.49 [c]	1035.76 [c]
d_1 [pa$^{0.5}$.m^3/mol]	-	-	-	3.575 [b]	1.806 [b]	0.907 [c]
d_2 [[d_1]*K$^{-0.5}$]	-	-	-	0.0938 [b]	0.018 [c]	0.119 [c]
σ × 10^{10} [m]	-	-	-	4.5 [a]	3.12 [a]	3.7 [a]
% AAD P_s	0.48	0.84	0.72	-	-	-
% AAD ρ_s	0.93	0.69	0.84	-	-	-
T_r range	0.45-0.88	0.48-0.9	0.73-0.99	-	-	-

a) Proposed from Huttenhuis et al. [6]
b) Re-adjusted in this work, the initial value is obtained from Medeiros et al. [14]
c) Adjusted in this work

Note : some values may be close to [14], but all (b) values have been re-adjusted in this work.

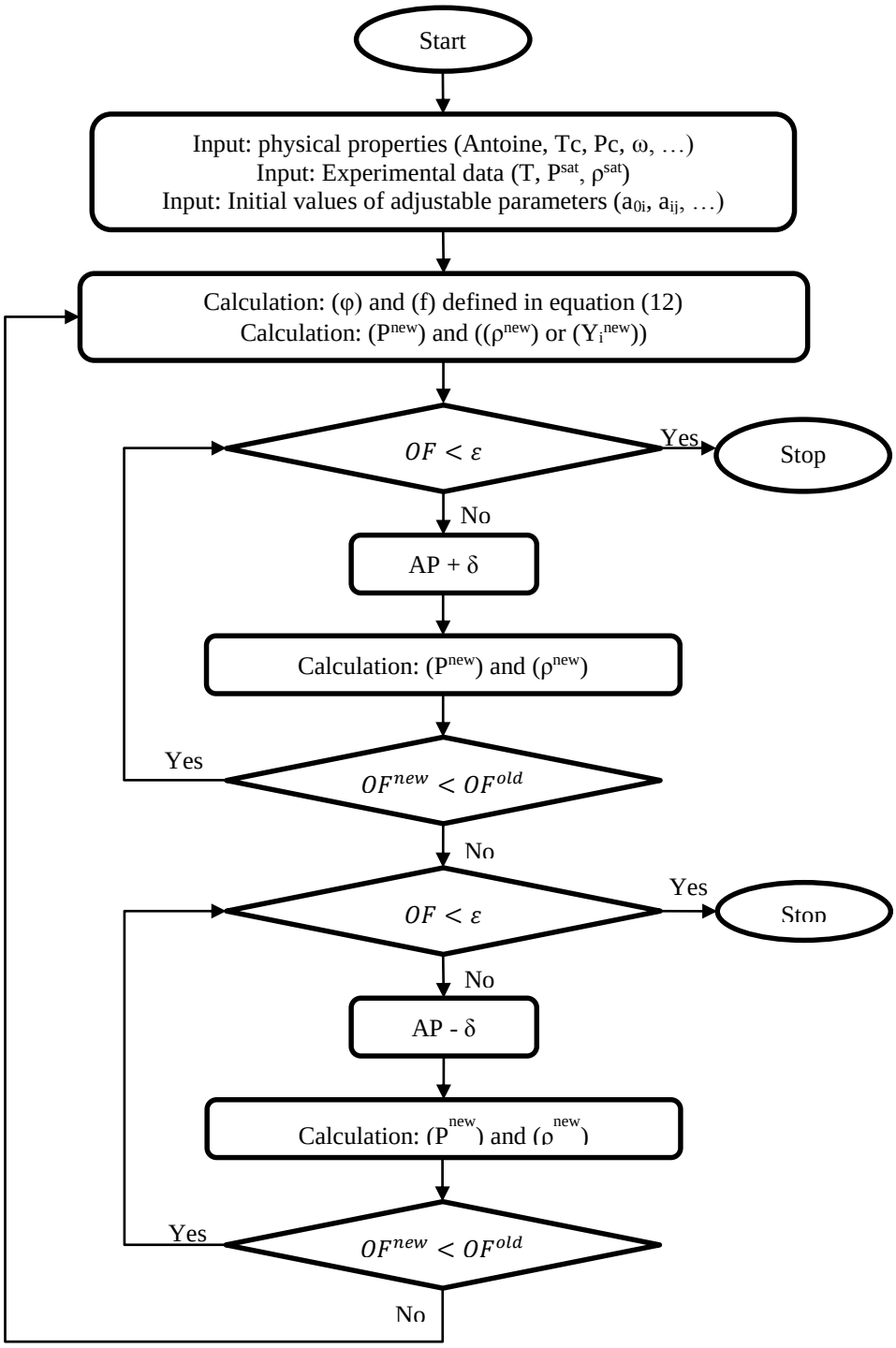

Figure 4. Adjustment algorithm of model parameters (Parameter optimization); AP = Adjustable parameters (Molecular & ionic component); OF = Objective function defined in equation 18, 19; δ = OF/100

4.2.2. Binary parameters

Before modeling the ternary system (H_2O-MDEA-CO_2), binary parameters for H_2O-MDEA and H_2O-CO_2 subsystems should be set. After adjusting the pure parameters, their values were fixed in the model and binary parameters were obtained based on them. The parameters of binary subsystems H_2O-MDEA and H_2O-CO_2 were adjusted through the objective function presented in Eq. (19). The algorithm used to minimize this objective function is presented in Fig. (4). Based on this, the average absolute percent deviation of model results compared to binary experimental

data was reduced to less than 1%. At each temperature a set of acceptable parameters was obtained. These parameters were included in the regressions to develop the model performance at different temperatures. Fig. (5) compares the vapor-liquid equilibrium data of binary subsystems H_2O-MDEA and H_2O-CO_2 obtained by the model and experimental data.

$$OF_{Binary} = OF_{Pure} + \sum\left(\frac{P_b^{cal}-P_b^{exp}}{P_b^{exp}}\right)^2 + \sum\left(\frac{Y_i^{cal}-Y_i^{exp}}{Y_i^{exp}}\right)^2 = Minimize \quad (16)$$

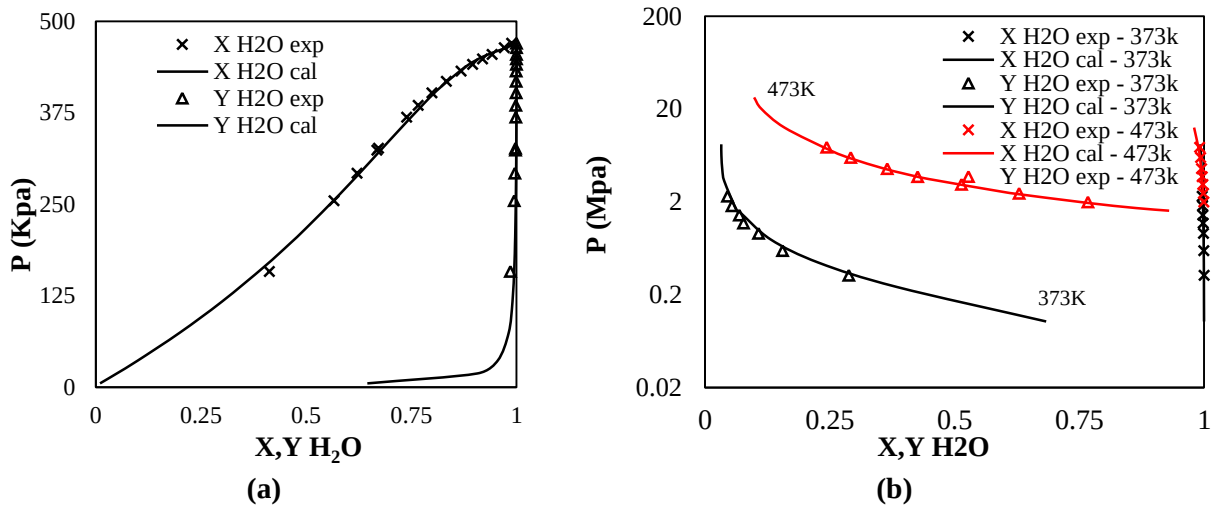

Figure 5. Vapor-liquid equilibrium data of binary systems : (a) VLE Data of H_2O-MDEA, (black lines) X_{H2O},and Y_{H2O} calculated by CTS^{DH} at 423K, (×) X_{H2O} experimental[26], (Δ) Y_{H2O} experimental[26]. (b) VLE Data of H_2O-CO_2, (black lines) X_{H2O}, andY_{H2O} calculated by CTS^{DH} at 373K, (red lines) X_{H2O}, and Y_{H2O} calculated by CTS^{DH} at 473K, (×) X_{H2O} experimental[29], (Δ) Y_{H2O} experimental[29].

The binary parameters of H_2O-Ions were optimized using the solubility data of the ternary system. The binary parameters obtained from the model as well as the experimental data used in this section are presented in Table (6).

Table 6.
Binary interaction parameters of the CTS^{DH}.

	E_{ij}	K_{ij}	AAD% (P_b)	AAD% (Y_i)	T (k)	Exp. Data
H_2O - MDEA	1866.44	- 0.179	1.31	0.18	293-458	25 - 28
H_2O - CO_2	834.34	- 0.083	0.98	0.47	313-623	29 - 32
H_2O – $MDEAH^+$	2532.96	- 0.011	-	-	-	This work
H_2O – HCO_3^-	999.7	0.0297	-	-	-	This work
H_2O – $CO_3^=$	1160.81	0.011	-	-	-	This work
MDEA - CO_2	1421.18	- 0.12	-	-	-	This work
MDEA - $MDEAH^+$	3116.06	- 0.0041	-	-	-	This work
MDEA - HCO_3^-	1580.14	- 0.197	-	-	-	This work
MDEA - $CO_3^=$	1742.75	- 0.36	-	-	-	This work
CO_2 - $MDEAH^+$	2088.21	0.21	-	-	-	This work
CO_2 - HCO_3^-	552.26	- 0.098	-	-	-	This work
CO_2 - $CO_3^=$	714.89	- 0.069	-	-	-	This work
$MDEAH^+$ - HCO_3^-	2246.44	0.026	-	-	-	This work
$MDEAH^+$ - $CO_3^=$	2409.08	- 0.073	-	-	-	This work
HCO_3^- - $CO_3^=$	873.12	- 0.037	-	-	-	This work

4.2.3. Modeling the ternary system

The results related to modeling the solubility of carbon dioxide in the N-methyldiethanolamine solution can be seen in this section. As mentioned earlier, in this work, the φ-φ method (CTS^{DH} EoS) is used to simultaneously solve VLE and chemical equilibrium calculations. To reduce the AAD% of the model, the calculations of the gas phase were also performed by the CTS EoS, although this action made the calculation time a little longer. The algorithm used in this work consists of two main loops: The calculation of P_t and Y_i in the inner loop and the calculation of the concentration of the species and α^{cal} in the outer loop. The calculation steps based on the mentioned algorithm are presented in Fig. (6).It is given in the following Eq. how to calculate the average absolute percent deviation (AAD%) (20).

$$AAD\% = \frac{100}{n_p}\sum_{i=1}^{n_p}\left|\frac{Exp - Cal}{Exp}\right| \qquad (17)$$

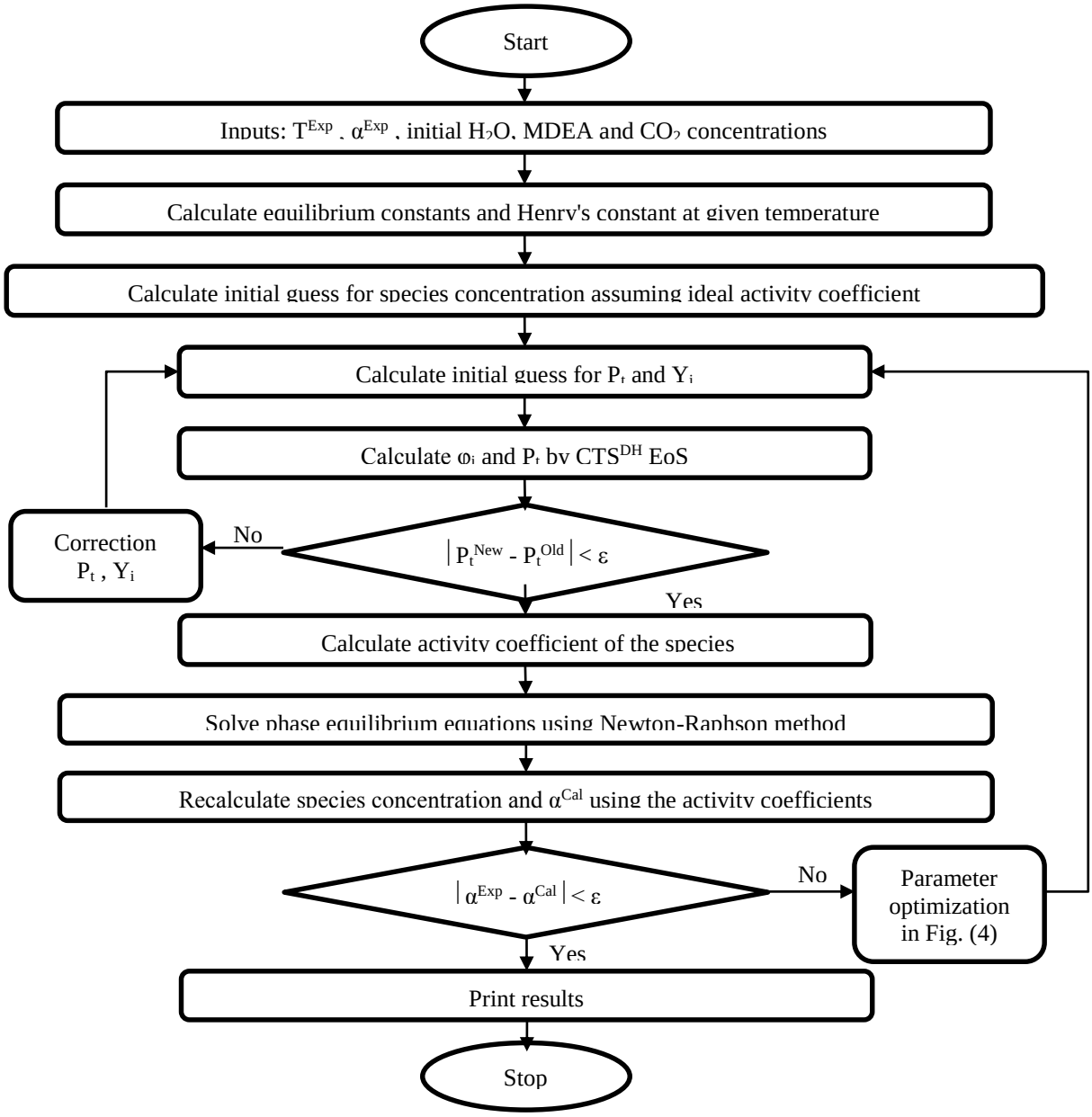

Figure 6. Solution algorithm to predict the concentrations of components and the CO_2 loading in the H_2O+MDEA+CO_2 system.

To check the experimental data and modeling results obtained from this work, the experimental data of twelve other articles were used[33-44]. Table (7) shows the reference literatures of the solubility of CO_2 in MDEA solutions used in this work.

Table 7.
Literature references of the solubility of CO_2 in aqueous MDEA solutions.

Author	Wt% $_{MDEA}$	T (K)	P_{CO2} (Kpa)	Ref.
Dash (2016)	22, 48	308-328	1 - 1400	[33]
Haji-Sulaiman (1998)	23.8, 47.3	303, 313, 323	0.1 - 98.2	[34]
Xu et al. (1998)	35.1, 39.8, 48.9	313, 323, 343, 353, 363, 373	0.9 - 1013	[35]
Bhairi (1984)	12, 24	25-115	14 - 4136	[36]
Jou et al., (1993)	35, 50	313, 373	0.004 - 236	[37]
Jou et al. (1982)	11.8, 23.4, 48.9	298, 313, 343, 373	0.001 - 6570	[38]
Ermatchkov (2006)	19.2, 32.3, 48.8	313-393	0.1 -70	[39]
Sidi-Boumedine (2004)	25.73, 46.88	298, 313, 348	2.84 - 4559.5	[40]
Rho et al. (1997)	5, 20, 50, 75	323, 348, 373	0.8 - 268.3	[41]
Derks (2010)	50	313	1.25 – 91.6	[42]
Ma'mun et al. (2005)	50	328, 343, 358	66 - 813	[43]
Park et al. (2001)	50	298, 323, 348, 373	0.8 - 140	[44]

The comparison of the results is shown in Fig. (7).

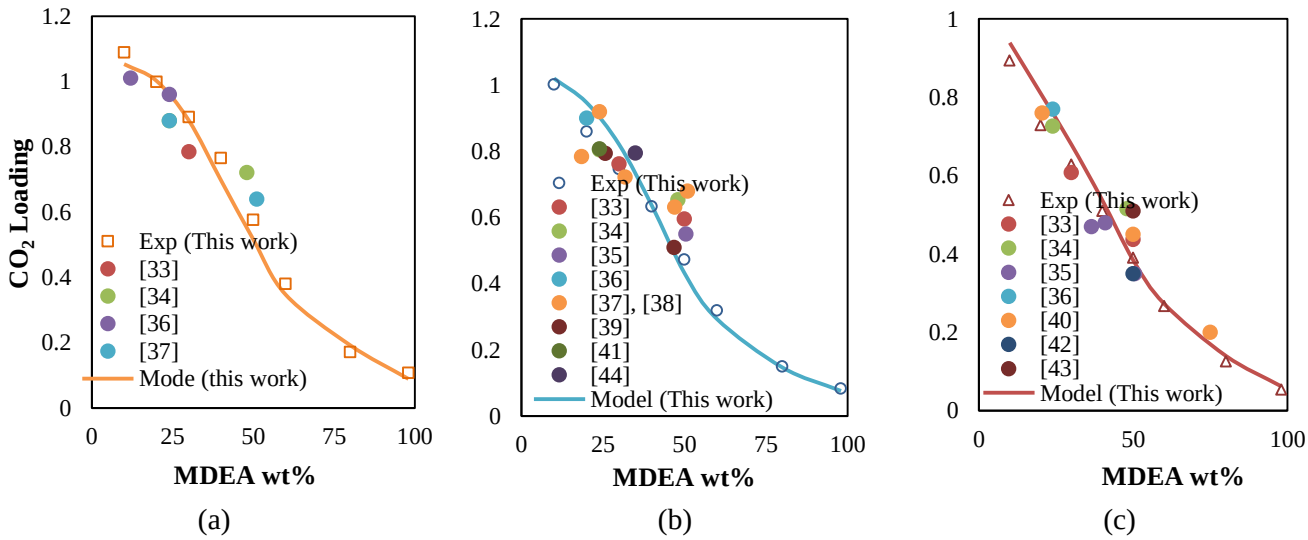

Figure 7. Comparison of experimental data (measured in this work) and the model (calculated by CTS^{DH}) CO_2 loading with the results of other researches for the H_2O-MDEA-CO_2 system at various temperatures and concentrations of MDEA at (a) 303.15 K, (b) 313.15 K, and (c) 323.15 K.

The total number of experimental points and the average absolute percent deviation (AAD%) recorded in this study are presented in Table (8).

Table 8.
Total number of experimental points and the average absolute percent deviation recorded in this study.

Components	Parameters	Comparison	Points	AAD%
H_2O	P^{sal}, ρ^{sat}	Exp^1 : Cal	42	0.7
MDEA	P^{sal}, ρ^{sat}	Exp^1 : Cal	46	0.76
CO_2	P^{sal}, ρ^{sat}	Exp^1 : Cal	40	0.78
H_2O - MDEA	P_t, Y_i	Exp^1 : Cal	30	0.74
H_2O - CO_2	P_t, Y_i	Exp^1 : Cal	20	0.72
H_2O - MDEA - CO_2	Loading	Exp^2 : Cal	72	7.05
H_2O - MDEA - CO_2	Loading	Exp^1 : Cal	34	13.50
Total	**-**	**-**	**284**	**-**

Exp^1: Experimental data of other researches
Exp^2: Experimental data in this work
Cal: calculated by CTS^{DH} (This work)

5. Conclusion

In this work, the solubility of carbon dioxide in 10-98 wt% of MDEA, at temperatures of 303-323K, and atmospheric pressure was measured and modeling of the system was taken place. In most of the experimental researches, the absorption of CO_2 in one or two specific concentrations of MDEA at constant temperature has been investigated. However, in this research, the absorption of CO_2 in eight different concentrations of MDEA (10-98% continuously) at constant temperature and pressure has been investigated, which can be one of the characteristics of the present work. As a result, the findings of this study can be used to select the optimal concentration of MDEA for gas absorption systems. As expected, the loading decreased by increasing temperature, which can be a confirmation of the correct procedure for conducting experimental studies in this work. Also, the mole of CO_2 absorbed by the solvent at a constant temperature increased by increasing the concentration of the solvent from 10 wt% to 40 wt%, but with a further increase in the concentrationof the solvent, the amount of absorption decreased. This can be related to the physicochemical properties of the solution (H_2O+MDEA). By increasing the concentration of MDEA in the mentioned Binary mixture, properties such as pH and viscosity change. At low concentrations of MDEA, the pH is low for absorption, and on the other hand, at high concentrations of MDEA, the high viscosity of the solution can be an obstacle for absorption. Therefore, the absorption of CO_2 will be optimal in intermediate concentrations. Of course, other factors can also be effective in determining the optimal concentration for absorption. The maximum moles of CO_2 were absorbed in the concentration of 40-50 wt% of MDEA, which increased from about 40% to about 50% as the temperature increased from 303K to 323K. Therefore, it can be said that the optimal concentration of MDEA increases slowly by increasing temperature. The CTS equation of state was improved in the electrolytic part and the existing parameters were re-adjusted. Some parameters that did not exist in previous literature,s were adjusted in this work. The results obtained from the model show that the CO_2 loading obtained from the model can replace the experimental data under a wide range of operating conditions. With the help of this modeling, the deviation of the model results from the laboratory data in the investigated range was reduced to 7.05%.

List of Abbreviations

AAD%: Average absolute percent deviation
OF: Objective function
Exp: Experimental value
Cal: Calculated value
VLE: Vapor-liquid equilibria
MDEA: N-methyldiethanolamine
MEA: Monoethanolamine
SRK EoS: Soave-Redlich-Kwong equation of state
TSAM: Two-State Association Model
CTS EoS: Cubic-Two-State equation of state
DH: Debye-Hückel
Wt%: Weight percent

List of symbols

x_i: Liquid mole fraction of component i
y_i: Vapor mole fraction of component i
α_{CO2}: CO_2 Loading (mole CO_2/mole MDEA)
φ: Fugacity coefficient
γ: Activity coefficients
K: Equilibrium constants
P: Pressure [Pa]
R: Gas constant (8.314) [m^3.pa/k.mol]
T: Temperature [K]
Z: Compressibility factor
Q: Volumetric flow rate of injectable solvent [ml/min]
V_{CO2}: Volume of CO_2 dissolved in the solvent [ml]
$U_{m,CO2}$: molar Volume of CO_2 [ml/mol]
a: Mixture dispersive parameter [m^6.pa/mole^2]
a': Derivative of the dispersion parameter
b: Co-volume parameter of CTS^{DH} [m^3/mol]
c: Parameter in the dispersion term
V: Characteristic association volume [m^3/mol]
E: Energy of association [m^3.pa/mol]
k_{ij}: Binary interaction parameter
d_1, d_2: Adjustable parameters in equation (22)
σ: Ion diameter [m]
f: Mayer function define in equation (11)
$\mathbb{X}$: Quantity define in equation (20)
$\acute{K}$: Inverse Debye screening length [1/m]
N_A: Avogadro's constant (6.02214076×10^{23}) [1/mol]
K_B: Boltzmann constant (1.380649×10^{-23}) [J/K]
ρ_N: Number density [1/m³], $\rho_N = (N_A.\rho/M_w)$
ε: Dielectric constant of the system [C^2/J.m]
e: Elementary charge (1.60219×10^{-19}) [C]
F: Faraday constant (96485) [C/mole]
$\hat{z}$: Charge number of ion
n_p: Number of experimental point
n: Number of mole

REFERENCES

[1] Kent, R. L., & Eisenberg, B. (1976). Better Data for Amine Treating.

[2] Posey, M. L., & Rochelle, G. T. (1997). A thermodynamic model of Methyldiethanolamine− CO2− H2S− Water. Industrial & engineering chemistry research, 36(9), 3944-3953. https://doi.org/10.1021/ie970140q.

[3] Deshmukh, R. D., & Mather, A. E. (1981). A mathematical model for equilibrium solubility of hydrogen sulfide and carbon dioxide in aqueous alkanolamine solutions. Chemical engineering science, 36(2), 355-362. https://doi.org/10.1016/0009-2509(81)85015-4.

[4] Fürst, W., & Renon, H. (1993). Representation of excess properties of electrolyte solutions using a new equation of state. AIChE Journal, 39(2), 335-343. https://doi.org/10.1002/aic.690390213

[5] Huttenhuis, P. J. G., Agrawal, N. J., Hogendoorn, J. A., & Versteeg, G. F. (2007). Gas solubility of H2S and CO2 in aqueous solutions of N-methyldiethanolamine. Journal of Petroleum Science and Engineering, 55(1-2), 122-134. https://doi.org/10.1016/j.petrol.2006.04.018.

[6] Huttenhuis, P. J. G., Agrawal, N. J., Solbraa, E., & Versteeg, G. F. (2008). The solubility of carbon dioxide in aqueous N-methyldiethanolamine solutions. Fluid phase equilibria, 264(1-2), 99-112. https://doi.org/10.1016/j.fluid.2007.10.020.

[7] Myers, J. A., Sandler, S. I., & Wood, R. H. (2002). An equation of state for electrolyte solutions covering wide ranges of temperature, pressure, and composition. Industrial & engineering chemistry research, 41(13), 3282-3297. https://doi.org/10.1021/ie011016g

[8] Cameretti, L. F., Sadowski, G., & Mollerup, J. M. (2005). Modeling of aqueous electrolyte solutions with perturbed-chain statistical associated fluid theory. Industrial & engineering chemistry

research, 44(9), 3355-3362. https://doi.org/10.1021/ie0488142

[9] Held, C., Cameretti, L. F., & Sadowski, G. (2008). Modeling aqueous electrolyte solutions: Part 1. Fully dissociated electrolytes. Fluid Phase Equilibria, 270(1-2), 87-96. https://doi.org/10.1016/j.fluid.2008.06.010.

[10] Held, C., & Sadowski, G. (2009). Modeling aqueous electrolyte solutions. Part 2. Weak electrolytes. Fluid Phase Equilibria, 279(2), 141-148. https://doi.org/10.1016/j.fluid.2009.02.015.

[11] Held, C., Sadowski, G., Carneiro, A., Rodríguez, O., & Macedo, E. A. (2013). Modeling thermodynamic properties of aqueous single-solute and multi-solute sugar solutions with PC-SAFT. AIChE Journal, 59(12), 4794-4805. https://doi.org/10.1002/aic.14212

[12] Held, C., Reschke, T., Mohammad, S., Luza, A., & Sadowski, G. (2014). ePC-SAFT revised. Chemical Engineering Research and Design, 92(12), 2884-2897. https://doi.org/10.1016/j.cherd.2014.05.017.

[13] Medeiros, M., & Téllez-Arredondo, P. (2008). Cubic two-state equation of state for associating fluids. Industrial & engineering chemistry research, 47(15), 5723-5733. https://doi.org/10.1021/ie071397j

[14] Téllez-Arredondo, P., & Medeiros, M. (2013). Modeling CO2 and H2S solubilities in aqueous alkanolamine solutions via an extension of the Cubic-Two-State equation of state. Fluid Phase Equilibria, 344, 45-58. https://doi.org/10.1016/j.fluid.2013.01.005.

[15] Debye, P., & Hückel, E. (1923). De la theorie des electrolytes. I. abaissement du point de congelation et phenomenes associes. Physikalische Zeitschrift, 24(9), 185-206.

[16] Pitzer, K. S. (1973). Thermodynamics of electrolytes. I. Theoretical basis and general equations. The Journal of Physical Chemistry, 77(2), 268-277. https://doi.org/10.1021/j100621a026

[17] Thomsen, K. (2009). Electrolyte solutions: Thermodynamics, crystallization, separation methods. DTU Chemical Engineering, Technical University of Denmark. https://doi.org/10.11581/dtu:00000073

[18] Breil, M. P. (2001). Thermodynamics, Experimental, and Modelling of Aqueous Electrolyte and Amino Acid Solutions. IVC-SEP, Department of Chemical Engineering, Technical University of Denmark.

[19] Pazuki, G. R., Pahlevanzadeh, H., & Ahooei, A. M. (2006). Solubility of CO2 in aqueous ammonia solution at low temperature. Calphad, 30(1), 27-32. https://doi.org/10.1016/j.calphad.2005.11.006.

[20] Pahlavanzadeh, H., & Farazar, M. (2009). Measurement and modeling of solubility of H 2 S in aqueous diisopropanolamine solution. Korean journal of chemical engineering, 26, 1112-1118. https://doi.org/10.1007/s11814-009-0185-8

[21] Soave, G. (1972). Equilibrium constants from a modified Redlich-Kwong equation of state. Chemical engineering science, 27(6), 1197-1203. https://doi.org/10.1016/0009-2509(72)80096-4

[22] Cerdeirina, C. A., Troncoso, J., Gonzalez-Salgado, D., García-Miaja, G., Hernandez-Segura, G. O., Bessieres, D., ... & Costas, M. (2007). Heat capacity of associated systems. Experimental data and application of a two-state model to pure liquids and mixtures. The Journal of Physical Chemistry B, 111(5), 1119-1128. https://doi.org/10.1021/jp0640272.

[23] American Institute of Chemical Engineers, Design Institute for Physical Properties, DIADEM, 2007.

[24] Kontogeorgis, G. M., & Folas, G. K. (2009). Thermodynamic models for industrial applications: from classical and advanced mixing rules to association

theories. John Wiley & Sons. https://doi.org/10.1002/9780470747537

[25] Soames, A., Al Helal, A., Iglauer, S., Barifcani, A., & Gubner, R. (2018). Experimental vapor–liquid equilibrium data for binary mixtures of methyldiethanolamine in water and ethylene glycol under vacuum. Journal of Chemical & Engineering Data, 63(5), 1752-1760. https://doi.org/10.1021/acs.jced.8b00054

[26] Na, J., Min, B. M., Moon, J. H., Lee, J. S., & Shin, H. Y. (2018). Isothermal Vapor–Liquid Equilibrium Data for Water+ Diisopropanolamine, Water+ N-Methyldiethanolamine and Diisopropanolamine+ N-Methyldiethanolamine Systems. International Journal of Thermophysics, 39, 1-12. https://doi.org/10.1007/s10765-018-2415-y

[27] Kim, I., Svendsen, H. F., & Børresen, E. (2008). Ebulliometric determination of vapor− liquid equilibria for pure water, monoethanolamine, n-methyldiethanolamine, 3-(methylamino)-propylamine, and their binary and ternary solutions. Journal of Chemical & Engineering Data, 53(11), 2521-2531. https://doi.org/10.1021/je800290k

[28] Voutsas, E., Vrachnos, A., & Magoulas, K. (2004). Measurement and thermodynamic modeling of the phase equilibrium of aqueous N-methyldiethanolamine solutions. Fluid Phase Equilibria, 224(2), 193-197. https://doi.org/10.1016/j.fluid.2004.05.012.

[29] Müller, G., Bender, E., & Maurer, G. (1988). Das Dampf-Flüssigkeitsgleichgewicht des ternären Systems Ammoniak-Kohlendioxid-Wasser bei hohen Wassergehalten im Bereich zwischen 373 und 473 Kelvin. Berichte der Bunsengesellschaft für physikalische Chemie, 92(2), 148-160. https://doi.org/10.1002/bbpc.198800036

[30] Takenouchi, S., & Kennedy, G. C. (1964). The binary system H 2 O-CO 2 at high temperatures and pressures. American journal of science, 262(9), 1055-1074.

[31] Kiepe, J., Horstmann, S., Fischer, K., & Gmehling, J. (2002). Experimental determination and prediction of gas solubility data for CO2+ H2O mixtures containing NaCl or KCl at temperatures between 313 and 393 K and pressures up to 10 MPa. Industrial & engineering chemistry research, 41(17), 4393-4398. https://doi.org/10.1021/ie020154i

[32] Chapoy, A., Mohammadi, A. H., Chareton, A., Tohidi, B., & Richon, D. (2004). Measurement and modeling of gas solubility and literature review of the properties for the carbon dioxide− water system. Industrial & engineering chemistry research, 43(7), 1794-1802. https://doi.org/10.1021/ie034232t

[33] Dash, S. K., & Bandyopadhyay, S. S. (2016). Studies on the effect of addition of piperazine and sulfolane into aqueous solution of N-methyldiethanolamine for CO2 capture and VLE modelling using eNRTL equation. International Journal of Greenhouse Gas Control, 44, 227-237. https://doi.org/10.1016/j.ijggc.2015.11.007.

[34] Haji-Sulaiman, M. Z., Aroua, M. K., & Benamor, A. (1998). Analysis of equilibrium data of CO2 in aqueous solutions of diethanolamine (DEA), methyldiethanolamine (MDEA) and their mixtures using the modified Kent Eisenberg model. Chemical engineering research and design, 76(8), 961-968. https://doi.org/10.1205/026387698525603

[35] Xu, G. W., Zhang, C. F., Qin, S. J., Gao, W. H., & Liu, H. B. (1998). Gas−liquid equilibrium in a CO2− MDEA− H2O system and the effect of piperazine on it. Industrial & engineering Chemistry research, 37(4), 1473-1477. https://doi.org/10.1021/ie9506328

[36] Bhairi, A. M. (1984). Experimental equilibrium between acid gases and ethanolamine solutions. Oklahoma State University.

[37] Jou, F. Y., Carroll, J. J., Mather, A. E., & Otto, F. D. (1993). The solubility of

carbon dioxide and hydrogen sulfide in a 35 wt% aqueous solution of methyldiethanolamine. The Canadian Journal of Chemical Engineering, 71(2), 264-268. https://doi.org/10.1002/cjce.5450710213

[38] Jou, F. Y., Mather, A. E., & Otto, F. D. (1982). Solubility of hydrogen sulfide and carbon dioxide in aqueous methyldiethanolamine solutions. Industrial & Engineering Chemistry Process Design and Development, 21(4), 539-544. https://doi.org/10.1021/i200019a001.

[39] Ermatchkov, V., Perez-Salado Kamps, A., & Maurer, G. (2006). Solubility of carbon dioxide in aqueous solutions of N-methyldiethanolamine in the low gas loading region. Industrial & engineering chemistry research, 45(17), 6081-6091. https://doi.org/10.1021/ie0604270

[40] Sidi-Boumedine, R., Horstmann, S., Fischer, K., Provost, E., Fürst, W., & Gmehling, J. (2004). Experimental determination of carbon dioxide solubility data in aqueous alkanolamine solutions. Fluid phase equilibria, 218(1), 85-94. https://doi.org/10.1016/j.fluid.2003.11.014

[41] Rho, S. W., Yoo, K. P., Lee, J. S., Nam, S. C., Son, J. E., & Min, B. M. (1997). Solubility of CO2 in aqueous methyldiethanolamine solutions. Journal of Chemical & Engineering Data, 42(6), 1161-1164. https://doi.org/10.1021/je970097d

[42] Derks, P. W. J., Hogendoorn, J. A., & Versteeg, G. F. (2010). Experimental and theoretical study of the solubility of carbon dioxide in aqueous blends of piperazine and N-methyldiethanolamine. The Journal of Chemical Thermodynamics, 42(1), 151-163. https://doi.org/10.1016/j.jct.2009.07.025

[43] Ma'mun, S., Nilsen, R., Svendsen, H. F., & Juliussen, O. (2005). Solubility of carbon dioxide in 30 mass% monoethanolamine and 50 mass% methyldiethanolamine solutions. Journal of Chemical & Engineering Data, 50(2), 630-634. https://doi.org/10.1021/je0496490

[44] Park, M. K., & Sandall, O. C. (2001). Solubility of carbon dioxide and nitrous oxide in 50 mass methyldiethanolamine. Journal of Chemical & Engineering Data, 46(1), 166-168. https://doi.org/10.1021/je000190t

[45] Press, W. H. (1992). Numerical recipes in Fortran 77: the art of scientific computing. Cambridge university press.